Uncertainty in classical systems
(with a local, non-stochastic, non-chaotic origin)

Mike R. Jeffrey[a]

(Dated: August 4, 2021)

Decisions made by two (or more) independent players in a dynamical system can result in an indeterminable, yet non-stochastic, outcome. The mechanism can be presented as a thought experiment in which two pilots attempt to steer a spacecraft but, in stabilizing its pitch and yaw, lose all knowledge of its forward motion. It is useful to think of this *pilots' dilemma* as a classical analogue of Schrödinger's "cat in a box" thought experiment. In both, the outcome of a life or death scenario is indeterminate until it is directly observed, but in place of the probabilistic radioactive source in Schrödinger's problem, the discontinuous action of the pilots' decisions create the classical indeterminacy. We discuss the wider implications of the phenomenon, such as predicting indeterminate scenarios in optimal transport or other network problems. The behaviour only becomes apparent when a systems dynamics is sufficiently taken into account.

[a] Engineering Mathematics, University of Bristol, Merchant Venturer's Building, Bristol BS8 1UB, UK, email: mike.jeffrey@bristol.ac.uk

I. INTRODUCTION

In this short paper we present a form of uncertainty that arises in classical systems due to switching between regimes of different behaviour. Viewing these regimes as different decision states, the phenomenon constitutes a macroscopic breakdown of the independence between two decisions, making their outcomes appear non-rational and ultimately indeterminable. The uncertainty has its origin neither in stochastic nor chaotic processes, nor is it due to deterministic non-rational behaviour. Instead it is geometrical in origin, arising due to a sensitivity to parameters, at the intersection of two or more thresholds where a choice is made between alternate regimes of dynamics.

The mathematical scenario we present is very general, but can be clearly expressed as a thought experiment. Two pilots are on a spaceship headed for Mars when their craft is crippled by some catastrophe. Their only means of control are a yaw thruster and a pitch thruster. One pilot will control each thruster, but their manual switches lie at distant ends of the ship, and with their electrics down they are unable to communicate. Can the pilots navigate their way to Mars successfully? We shall show that in successfully steering towards Mars, the pilots lose all knowledge of their forward acceleration, and hence any ability to safely complete their mission.

An instructive comparison can be made with Schrödinger's thought experiment illustrating quantum uncertainty [20]. In this, the life or death of a cat inside a box is determined by whether a radioactive source decays and triggers the release of a poison. Subject to the laws of quantum mechanics, the cat cannot be determined as either alive or dead until it is directly observed upon opening the box. In our problem it is instead the pilots' fate at stake, as the outcome of their decisions on the ship's forward motion is indeterminable despite knowing their individual behaviours at any instant. We shall make a closer comparison once we have described the phenomenon of interest.

When the physical conditions determining a system's state change abruptly, we observe these as discontinuities in the equations governing their evolution. Discontinuities lead to indeterminacies in a system's solutions, but these are often resolvable by more precise modeling. We shall show that there are certain situations where more precise modeling will fail to resolve the indeterminacy, as an in*stability* renders the outcome sensitive beyond all orders to the slightest perturbation.

In the context of the stricken spaceship, each pilot is able to apply an appropriate sequence of thrusts to achieve their required pitch and yaw. It is clear that their precise pattern of incremental thrusts may be rather complex, but it is less clear that their forward motion will turn out to be entirely indeterminable, becoming infinitely sensitive to everything from the precise processes and sequences of decision making to the behaviour of the thrusters.

There are many alternative ways we might have formulated the problem that point to likely real world applications that involve decision making, control switching, or routing problems. A particularly general set up is to consider the transport of two resources across a network, with the choice of how to route the two resources taking the place of the pilot's decisions, creating an indeterminacy in outcomes that would not be obvious in the usual ways of setting up an optimal transport problem.

We briefly discuss transport and other related problems section V. In section II we set up the piloting game to illustrate the phenomenon, before providing an overview explanation from macro and micro scopic perspectives in section III and section IV.

II. THE PILOTS' DILEMMA

Let us set down equations for the scenario of the pilots' dilemma. Let u and v represent the pitch rate and yaw rate of a spaceship, respectively, and w represent its forward velocity. The ship's two pilots will attempt to stabilize the pitch and yaw rates, presumably around a desirable absolute orientation. We shall assume the pilots respond to these rates of change by thrusting to counteract any motion heading away from their desired trajectory.

With a vector $\mathbf{u} = (u, v, w)$ giving the rates of pitch, yaw, and forward motion, respectively, the actions of the pilots take the form of an acceleration $B_{\mathbf{u}} = (B_u, B_v, B_w)$ applied by the thrusters (using 'B' because these will be made up of Boolean decision functions).

These accelerations depend on the current thrust mode at any moment as decided by the pilots. To encode these decisions we will define two Boolean variables,

$$\lambda_u = \text{step}(u - u_*) \quad \& \quad \lambda_v = \text{step}(v - v_*) \ , \tag{1}$$

where u_* and v_* are desirable thresholds at which to switch the thruster modes, and 'step' is the Heaviside step function (1 for positive argument and 0 for negative, and for now we leave step(0) defined only as lying between 0 and 1). The accelerations will then be given by functions $B_{\mathbf{u}} = B_{\mathbf{u}}(\lambda_u, \lambda_v)$ of these Boolean variables. It is easy to see that these functions take the form

$$\begin{aligned} B_{\mathbf{u}}(\lambda_u, \lambda_v) \ &= \ \lambda_u(1-\lambda_v)B_{\mathbf{u}}(1,0) \ + \ \lambda_u\lambda_v B_{\mathbf{u}}(1,1) \\ &\quad + (1-\lambda_u)\lambda_v B_{\mathbf{u}}(0,1) \ + \ (1-\lambda_u)(1-\lambda_v)B_{\mathbf{u}}(0,0) \ , \end{aligned} \tag{2}$$

such that plugging in λ_u and λ_v as 0 or 1 on the righthand side yields the appropriate decision output $B_{\mathbf{u}}(0,0), B_{\mathbf{u}}(1,0), B_{\mathbf{u}}(0,1)$, or $B_{\mathbf{u}}(1,1)$.

This allows us to write the acceleration resulting from the pilots' decisions as

$$\tfrac{d}{dt}\mathbf{u} = B_{\mathbf{u}}(\lambda_u, \lambda_v) \ . \tag{3}$$

A factor multiplying the term 'λ_u' in (2) represents an action taken if the craft is pitching upward, while a factor multiplying the term '$1 - \lambda_u$' represents an action taken if pitching downward, and so on, so that the coefficients in (2) constitute logical terms as summarized in fig. 1, while the overall function $B_{\mathbf{u}}$ provides the thrust they result in.

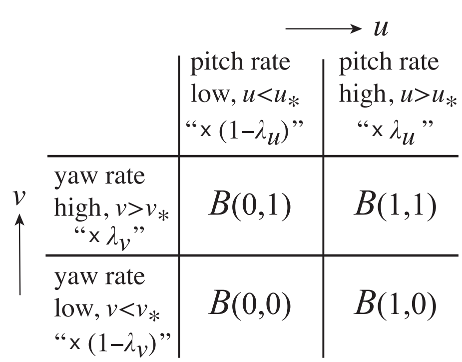

FIG. 1. Boolean terms that contribute to each $B(\lambda_u, \lambda_v)$.

The expressions (2) and (3) will be useful in a number of ways. Note, however, that

(3) describes only the instantaneous thrust, and will not describe the acceleration over a sustained period of motion, which instead requires a different set of equations.

Say that, over a given duration, the thrusters spend a fraction of time μ_{ij} in each mode $B(i,j)$, then the motion is given by

$$\tfrac{d}{dt}\mathbf{u} = \mu_{11}B_{\mathbf{u}}(1,1) + \mu_{10}B_{\mathbf{u}}(1,0) + \mu_{01}B_{\mathbf{u}}(0,1) + \mu_{00}B_{\mathbf{u}}(0,0) \ , \tag{4}$$

with a normalization condition $\mu_{11} + \mu_{10} + \mu_{01} + \mu_{00} = 1$.

We may describe (3) and (4) as the microscopic and macroscopic equations of motion, respectively. While the motions follow (3) at each instant, over any interval of time the motion must instead follow (4), and only under special conditions are the two equivalent.

It is with equation (4) that the fate of our pilots is placed in jeopardy. Their first objective is to stabilize their pitch and yaw motion to $u = u_*$ and $v = v_*$, and hence achieve

$$\tfrac{d}{dt}(u,v) = (0,0) \ . \tag{5}$$

According to (4), there are three unknowns μ_{11}, μ_{10}, μ_{01}, (with one fixed by the normalization condition $\mu_{00} = 1 - \mu_{11} - \mu_{10} - \mu_{01}$). Only two of these μ_{ij}s are fixed by (5), leaving one undetermined. This leaves the remaining equation of motion $\frac{dw}{dt}$ in (4) able to take a range of possible values, lying in a one-dimensional set parameterized by the remaining undetermined μ_{ij}. The ship's forward acceleration is thus uncertain.

This is not so surprising, since despite the microscopic equations of motion (3) being well-determined, for the macroscopic motion we have constructed a problem with two constraints and three unknowns. The non-trivial problem arises because this indeterminacy arises in what constitutes a singular limit: there is no unique well-determined 'regularization' of this system that will resolve it. If we attempt to model the processes behind the pilots' decision, we shall find a whole range of possible models all consistent with the same limits (3) and (4), and yet with inconsistent outcomes.

This is concerning, as such a scenario can arise in any process of interacting decisions that are instantaneously given by an equation like (3), but over long times are described by (4). Equations like these, with discontinuous terms representing abrupt systemic changes governing how a state evolves, are increasingly common in a broad range of disciplines, from friction to genetics to economics. Discontinuous quantities like (1) may represent anything from decisions to transitions between different media with different physical properties; we will remark further on applications at the end of this article. For more than two decisions or discontinuities, moreover, the problem only worsens, but two will be enough for us here.

The pilots' goal is to to stabilize the pitch and yaw motion, and for this to be possible we must have (at least locally)

$$B_u(1,\cdot) < 0 < B_u(0,\cdot) \ , \qquad B_v(\cdot,1) < 0 < B_v(\cdot,0) \ . \tag{6}$$

where the '$\cdot$' denotes a 0 or 1. We can assign arbitrary values to the forward acceleration $B_w(\cdot,\cdot)$. For illustration we will take

$$\begin{aligned} B_{\mathbf{u}}(0,1) &= \tfrac{1}{10}(5,-3,13) \ , \qquad & B_{\mathbf{u}}(1,1) &= \tfrac{-1}{10}(2,3,3) \ , \\ B_{\mathbf{u}}(0,0) &= \tfrac{1}{10}(5,7,-5) \ , \qquad & B_{\mathbf{u}}(1,0) &= \tfrac{1}{10}(-8,7,-7) \ . \end{aligned} \tag{7}$$

These values are not special, and similar behaviour will be observed with randomly chosen coefficients; these have merely been tuned slightly to highlight certain aspects of the behaviour. We have taken constants in (7) for simplicity, but these could involve functions of the displacements, velocities, and even time, provided locally the conditions (6) are satisfied.

It is important that the four vectors $B_{\mathbf{u}}(0,1)$, $B_{\mathbf{u}}(1,1)$, $B_{\mathbf{u}}(0,0)$, $B_{\mathbf{u}}(1,0)$, are linearly independent. If they are not, the coefficients μ_{ij} will be uniquely determined by (5) (because linear dependence will fix another μ_{ij}) and so the motion will be well-determined. This means that the indeterminacy of interest arises when the pilots' decisions are not simply additive: it is necessary at least that the pitch thruster has some effect on the yaw motion, or vice versa, and that they both affect the forward motion in a non-additive way (so both thrusters firing together produce more or less acceleration than firing separately, perhaps due to power limitations). These create a kind of nonlinearity, specifically the presence of the bilinear $\lambda_u \times \lambda_v$ term in (3). This affects the rational interpretation of the pilots' actions, as we discuss in section III.

Let us start with a simple experiment, a numerical simulation that works by solving (3) in discrete time steps. Suppose that the thrusters fire in $\delta t = 6$ minute intervals. The accelerations are piecewise-constant, so the velocity simply updates as

$$\mathbf{u}(t+\delta t) = \mathbf{u}(t) + \delta t . B_{\mathbf{u}}(\lambda_u, \lambda_v) \ . \tag{8}$$

Let the pilots decide how to set the thrusters at the same time once every hour (i.e. every $\Delta t = 60$ minutes, or every 10 thrusts). In the lefthand graph of fig. 2 we plot the the absolute pitch x and yaw y (the integrals of u and v), which successfully stabilize to $x \approx y \approx 0$. Curve (i) shows the corresponding forward displacement z (the integral of w): the ship is accelerating forwards.

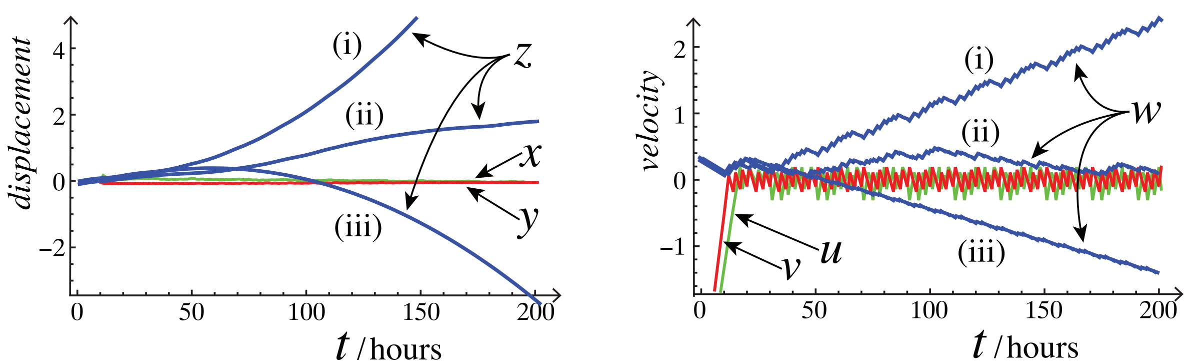

FIG. 2. Graphs of displacement and velocity from a discrete time simulation. Graphs of z and w are shown for the different decision models (i)-(iii) described in the text. Graphs of x, y, u, v, are shown for case (i) (and indistinguishable for (ii)-(iii); units are in radians and radians per hour). The small offsets used to stabilize x and y are $v_* = -0.007$, with $u_* = +0.0025$ in (i) and $u_* = -0.002$ in (ii-iii) (this stabilizes the displacement but is not significant for the variability in velocities). Initial conditions are $\mathbf{x} = (0.1, 0.07, 0)$ and $\mathbf{u} = (-1,-1,1)\frac{\pi}{10}$.

If we change the timing of decisions there is no visible difference in the graphs for x and y, but the graph for z changes markedly. Curve (ii) shows the outcome if the pitch is instead reset every 9 thrusts, and curve (iii) if the yaw is instead set every 9 thrusts (while in each case the opposite thruster is still reset every 10 thrusts). The corresponding velocities are shown in the righthand graph, with u and v stabilizing to around zero (with the chatter of the decisions across the decision thresholds clearly visible), while w varies substantially. The acceleration (i.e. gradient) along the three curves is approximately: (i) $+11.7$, (ii) -0.95, (iii) -8.31, in metres per hour squared.

The timings of the pilots' decisions markedly affect the ship's forward motion, despite its pitch and yaw hardly changing between the different implementations. In (i) the pilots make their decisions after every 10 thrusts, in (ii) and (iii) they make them every 9^{th} or 10^{th} thrust.

If we decrease the timestep δt between thrusts, and even let it tend to zero, the different between the pilot behaviours in (i)-(iii) becomes infinitesimal, yet the difference in the graphs for (i)-(iii) in fig. 2 remain unchanged, and hence contradictory. This is the singular limit — no matter how perfectly we try to simulate or sample the motion, infinitesimal changes in the pilots' decision making will give entirely different outcomes. And so far we have only considered a rather ideal discrete problem.

Figure 3 shows estimates of the acceleration for a range of models that constitute other small perturbations of the decision making process. The white 'hull' region (between the grey borders) shows the set of all behaviours that are physically possible, formed from the convex hull of all accelerations permitted by (4) as each μ_{ij} varies between 0 and 1.

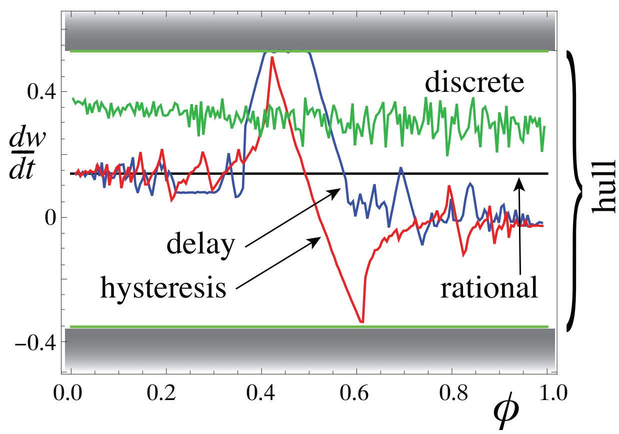

FIG. 3. Simulations of $\frac{dw}{dt}$ for different decision models: discrete model (8) with both pilots making decisions every ϕ hours; rational model (12) treating $\{\lambda_u, \lambda_v\}$ as independent macroscopic probabilities; hysteretic across the decision boundaries of size $\delta u = \varepsilon_u$, $\delta v = \varepsilon_v$, or time delay across the decision boundaries of size $\delta t = \varepsilon_u$ across $u = u_*$ and $\delta t = \varepsilon_v$ across $v = v_*$, with $\varepsilon_v/\varepsilon_u = \tan\frac{\pi\phi}{2}$ in both cases.

The 'rational' curve in fig. 3 shows the value of $\frac{dw}{dt}$ obtained if we apply the equations (5) assuming that the microscopic equation (3) holds over a long time scale, treating λ_u and λ_v as continuous variables (we shall say more about this interpretation in section III). This can also be interpreted as the game theoretical equilibrium solution if the two pilots are players in a competitive game (see e.g. [10, 18]), or the outcome if the thrusts switch on/off as step functions but instead smoothly via steep sigmoid functions. In each of these we treat λ_u and λ_v essentially as continuous variables between 0 and 1, and seek their values when (3) satisfies (5), which has a unique solution.

The remaining graphs in fig. 3 model the decision making process as having a spatial or temporal delay between the crossing of the thresholds $u = u_*$ and $v = v_*$, and the resetting of the thruster modes. The 'discrete' curve just simulates each pilot choosing the thruster settings each time a thruster is fired, similar to fig. 2 but at intervals of $\delta t = \Delta t = \phi$ hours. The 'hysteresis' curve assumes that the pilots react after an overshoot ε_u and ε_v in the u and v values themselves, while the 'delay' curve assumes the pilots react at times ε_u and ε_v after u or v pass their desired values, and we characterize these by their ratio $\varepsilon_v/\varepsilon_u = \tan\frac{\pi\phi}{2}$.

The graphs are generated by running each simulation for long enough that the dynamics finds an attractor around $u \approx u_*$, $v \approx v_*$, then reading off the proportions μ_{ij} of time spent in each mode $B_{\mathbf{u}}(\cdot,\cdot)$ in the attractor, and using (4) to calculate the effective $\frac{dw}{dt}$.

As before, we can shrink the absolute size of the discretization steps or the overshoots in these models to zero, whereupon the differences between the models become infinitesimal, and yet the difference in their outcomes will remain unchanged. The outcome is sensitive beyond all orders to the precise way decisions are taken and implemented.

We should emphasize that the erraticness of the graphs in fig. 3, and disagreement between them, is not an effect of inherent randomness in the system, as so far no randomness or noise is present. To further demonstrate this we can add noise, either as random perturbations of the state at each discretization step, or random perturbations of the time delays, resulting in fig. 4. Noise dampens down the level of volatility seen in fig. 3, and pushes solutions to the 'rational' outcome. The spatial noise is a perturbation of the discrete model, and we see that for very small noise the 'discrete' curve from fig. 3 is just slightly flattened, but for larger noise it collapses towards the 'rational' outcome. This shows that the sensitivity in the system is indeed due to a geometric instability, not any underlying randomness. It also hints — somewhat loosely — that the volatility of the system is linked to a loss of rationality in interaction of the pilots' decisions.

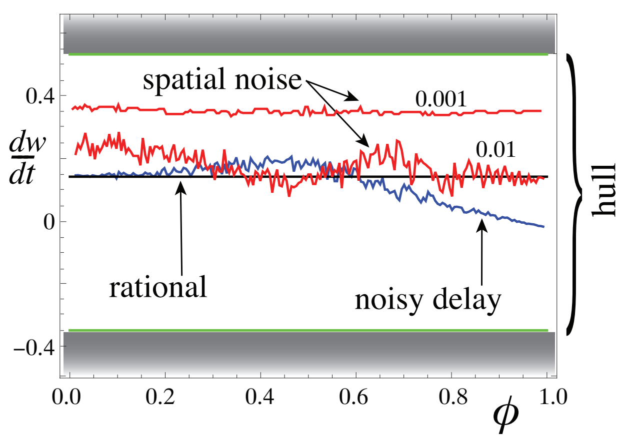

FIG. 4. The discrete simulation from fig. 3 with random perturbations to the velocity of amplitude 0.001 or 0.01 (as indicated) at each time step, and the delay simulation from fig. 3 with the delay multiplied by a random factor between 0 and 1 each time a decision threshold is crossed. The hull an rational curve are reproduced for reference.

III. PROBABILISTIC EXPLANATION

In (4) we introduced four macroscopic quantities μ_{ij}, which were the overall proportion of time for which the ship had its pair of thrusters in each overall mode 'ij' during its motion. We can instead assign a probability, ρ, that *each* thruster is in its '1' mode at any instant, i.e.

$$\rho_u = \text{probability that } u > u_* \;, \qquad \rho_v = \text{probability that } v > v_* \;, \tag{9}$$

which we may write as $\rho_u = \text{Prob}(u > u_*)$ and $\text{Prob}(v > v_*)$. It must then be true that

$$\rho_u = \mu_{10} + \mu_{11} \ , \qquad \rho_v = \mu_{01} + \mu_{11} \ , \tag{10}$$

or in lengthier notation,

$$\text{Prob}(u > u_*) = \text{Prob}(u > u_* \ \cap \ v > v_*) + \text{Prob}(u > u_* \ \cap \ v < v_*) \ ,$$

and

$$\text{Prob}(v > v_*) = \text{Prob}(u > u_* \ \cap \ v > v_*) + \text{Prob}(u < u_* \ \cap \ v > v_*) \ .$$

So while μ_{11} gives the probability that the pair of thrusters are both in the '11' setting, ρ_u and ρ_v give the separate probabilities that each individual thruster is in the '1' setting. The usual laws of logic tell us how to combined these. It appears in our problem that the pilots act independently. If the probabilities ρ_u and ρ_v are independent then it is also true that $\text{Prob}(u > u_* \ \cap \ v > v_*) = \text{Prob}(u > u_*) \times \text{Prob}(v > v_*)$, or in our notation

$$\mu_{11} = \rho_u \rho_v \ . \tag{11}$$

Substituting (10) and (11) into the macroscopic equations (4) return us (after a little straightforward algebra) to the microscopic equations

$$\tfrac{d}{dt}\mathbf{u} = B_{\mathbf{u}}(\rho_u, \rho_v) \ , \tag{12}$$

just with the binary variables $\lambda_{u,v} = 0$ or 1 replaced by continuous probabilities $\rho_{u,v} \in [0, 1]$. That is, while $\lambda_{u,v}$ represented decision states, $\rho_{u,v}$ now represent the probability that the system is in each of those states at any time.

Applying the conditions (5) then provides two conditions that uniquely fix the values of the probabilities ρ_u and ρ_v for which the ship's course stabilizes. This is the 'rational' curve in fig. 3, namely the rational outcome of the pilots' decisions if they can be treated as independent. If (11) holds for the macroscopic probabilities μ_{ij} and $\rho_{u,v}$, then the rational behaviour at any instant given by (3) or (12), is equivalent to the observed macroscopic behaviour (4).

Alas, in our simulations we find that although the pilots' instantaneous decisions are made independently, this independence does not carry over to their macroscopic behaviour. That is, (10) is found to hold, but (11) does not, and as a result (4) does not simplify to (2). The quantities calculated from the discrete simulations from fig. 2 listed in table I show this. The fact that the pilots act independently does not translate to independence of the probabilities ρ_u and ρ_v, that their thrusters are in any given mode during their motion.

experiment	ρ_u	ρ_v	$\rho_u\rho_v$	μ_{11}	μ_{10}	μ_{01}
(i)	0.468	0.472	0.221	0.149	0.318	0.323
(ii)	0.549	0.490	0.269	0.290	0.259	0.200
(iii)	0.557	0.431	0.240	0.360	0.196	0.070

TABLE I. The probabilities ρ_u, ρ_v, and μ_{ij}, calculated from the simulations (i-iii) from fig. 2 (recall that $\mu_{00} + \mu_{10} + \mu_{01} + \mu_{11} = 1$). Note that (10) holds but (11) does not.

IV. MICRO-DYNAMIC EXPLANATION

The source of erratic variation in the outcome of decisions is fairly simple to explain as a general mechanism. The specific details for any given model of the decision processes are very intricate, however, and only partially understood. When u and v stabilize to values $u \approx u_*$ and $v \approx v_*$, they are actually evolving around a small but complex attractor in the neighbourhood of the decision thresholds. A sample of these attractors are simulated in fig. 5 using different decision processes from fig. 3. Before we go on to discuss these in more detail, for now note simply how the dynamics in the (u, v) plane, close to the decision thresholds, varies drastically between different decision models. In (i.a-c) there is a hysteretic overshoot in u and v before the pilots react, and as we change the relative overshoots of the two pilots, the system evolves around an attractor with markedly different shape and periodicity (or chaos). Similar differences are seen in fig. 5(ii.a-c) in the time-delayed model, as the relative time delays in the pilots' decisions is varied. The attractors formed by other processes are more complex and their bifurcations less obvious, but examples of these attractors are shown, simulating decisions in a discretized model in (iii), with a randomly chosen time delay in (iv), or with a discretized model subject to random spatial perturbations in (v).

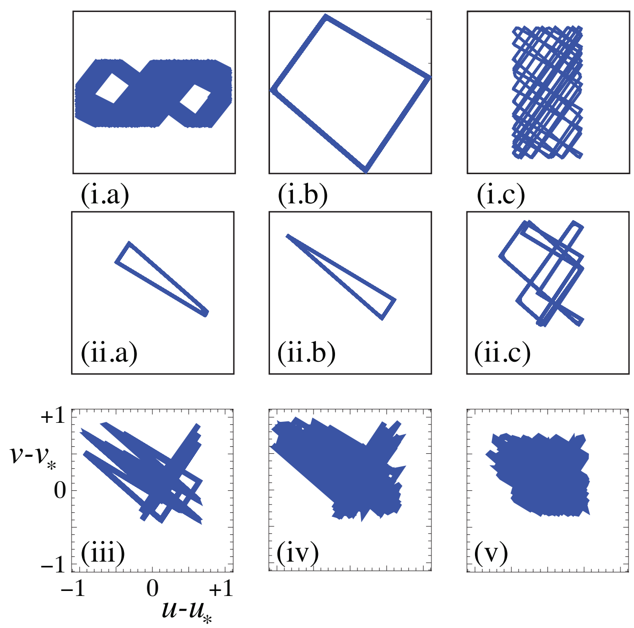

FIG. 5. Attractors formed in an ε-neighbourhood of $u = u_*$, $v = v_*$, if the pilots' decisions involve: (i) hysteresis with ϕ values a) 0.3, b) 0.5, c) 0.7; (ii) time delay with ϕ values a) 0.4, b) 0.5, c) 0.65; (iii) discretization with $\phi = 1$; (iv) noisy time delay with $\phi = 1$; (v) spatial noise with $\phi = 1$.

To make this clearer, in fig. 6 we show the attractors in the first two rows of fig. 5, along with the points on the graphs in fig. 3 they are responsible for. We see how, as we move along the graphs, the shape and period of the attractors change markedly. The attractors are undergoing bifurcations, marked by the abrupt changes in gradient of the graphs, i.e. by how the forward acceleration $\frac{dw}{dt}$ changes with the parameter.

More in-depth but abstract investigations of these attractors and their bifurcations can be found in [12–14]. In fact the first hints of the bifurcations behind this (in the setting of hysteresis) date back to [3], but their full significance took longer to be realised, and

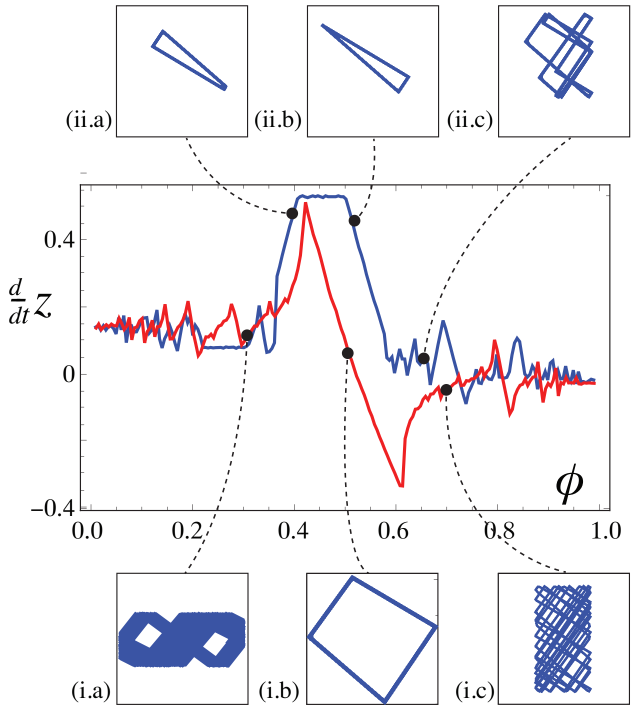

FIG. 6. The hysteresis and delay graphs from fig. 3, showing the attractors from fig. 5 that give rise to them, at three sample points each.

in-depth analysis has only been possible so far for a small sample of the possible decision processes. We shall summarise what is known.

The hysteretic case is the easiest to study in detail, as is done in [3, 14]. Because there is a spatial overshoot of ε_u and ε_v before switching occurs over the thresholds $u = u_*$ and $v = v_*$, the dynamics bounces around inside a 'chatterbox' with edges $u = u_* \pm \varepsilon_u$ and $v = v_* \pm \varepsilon_v$, forming a one-dimensional map (in the space of (u, v)). An example is shown in fig. 7(left). Although this map is discontinuous, its second return map is continuous, but non-differentiable anywhere a trajectory enters or exits a corner of the chatterbox; an example with the corresponding orbit is shown in fig. 7(right). At each parameter there exists a unique periodic or chaotic attractor (like those in fig. 5(i) and fig. 7). Whenever the attractor touches the corner of the chatterbox, corresponding to touching a vertex of the one-dimensional return map, a *discontinuity-induced* bifurcation occurs, in which their period and shape can jump abruptly. This causes an aprupt change in the portions of time μ_{ij} spend in each thruster mode, resulting in an abrupt change in the forward w dynamics.

For the other decision processes in fig. 3, the explanation for the erraticness of the predicted speeds is analogous, but more complex. In any case the dynamics in the (u, v) plane in the neighbourhood of the thresholds $u = u_*$, $v = v_*$, is given by a two-dimensional non-differentiable map. These can undergo a vast array of abrupt changes through discontinuity-induced bifurcations that occur at non-differentiable points of their maps, understood in two dimensions or above only in special cases, such as the border collision maps [7, 21].

A detailed analysis of each possible decision process, while no doubt illuminating, is not necessary to understand the main point. As in the hysteretic case, we see that these discontinuity-induced bifurcations constitute an abrupt change in the sequencing and timing of decisions near the cross-hairs of the u and v decision thresholds. Each bifurcation results

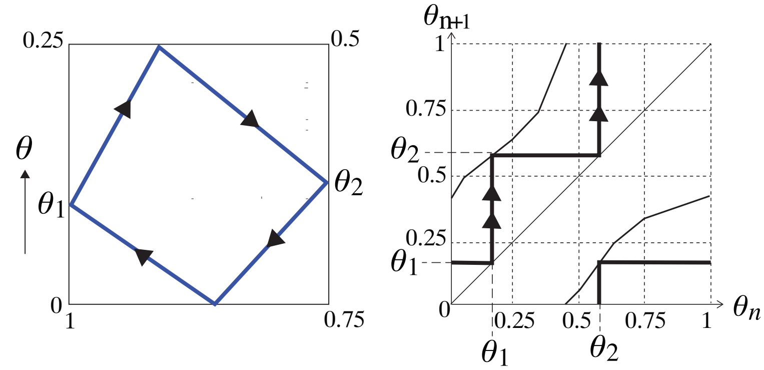

FIG. 7. The decision dynamics in the neighbourhood of $u = u_*$, $v - v_*$, for a hysteretic decision process, is described in (u, v) space by a one-dimensional map on the boundary of the *chatterbox* (left) on which decisions are implemented. We take a coordinate $\theta \in [0, 1)$ around the boundary of the chatterbox. The second return map (right) is a piecewise linear map on the circle. An example orbit is shown on each.

in an aprupt change in the proportion of time μ_{ij} spends in each thruster mode, resulting in abrupt changes in the forward w dynamics. Moreover between the different decision processes the kinds of attractors formed, and hence the proportions μ_{ij} and forward motion, are markedly different. If we proceed towards an ideal limit, letting the time between decisions tend to zero, occurring infinitesimally close to the ideal decision threshold, the difference between these decision processes becomes infinitesimal, and yet makes no difference to volatility of the forward (z) dynamics.

The sensitivity of the dynamics arises because these bifurcations are closely spaced with respect to parameter variations, as seen in fig. 5 by the closeness of non-differentiable edges in the graphs of $\frac{dw}{dt}$ varying with the parameter ϕ. Similar graphs would be obtained if we varied other parameters in the model, for example the thruster constants in (7). We could, for instance, extend the simulations in fig. 2 to produce a graph similar to fig. 3, in which ϕ represents the difference in the pilots' relative timings due to hysteresis, and we could plot the specific attractors similar to fig. 5 behind each observed acceleration.

The simulated processes here are motivated by a range of applications. Economics and biology often use discrete models, stepping between freeze-frames in a system's motion. Computer simulations are necessarily discrete. In such models a decision can be enacted at a given step without any obvious consequences for determinacy becoming apparent. Delay and hysteresis are particularly of concern in electronic control and rigid body mechanics. A popular current trend, to facilitate numerical or analytical analysis, is to approximate discontinuous quantities like (1) with smooth sigmoid functions, in the assumption this results in a well-defined 'regularized' system. We see here how these approaches would all give seemingly sensible and yet contrary resolutions to the same problem, due to an underlying and unobvious instability. The danger is that a very rigorous study in any one of these settings would give the illusion of uniqueness, when in fact exercising only selectivity among the infinities of a fundamentally indeterminate and sensitive problem. In many applications it is likely that various such practical factors are involved, i.e. elements of discretization, delay, hysteresis, and noise, all competing to make the indeterminacy of the pilots' dilemma unresolvable. It is therefore important to understand when such ambiguities exists in the first place, and just how sensitive they make the outcome.

V. APPLICATIONS, AND RELATIONS TO OTHER KINDS OF INDETERMINACY

The decisions made by the pilots in this problem constitute discontinuities which, though this thought experiment is classical and non-stochastic, render the pilots' fate indeterminable. The rationalilty of their independent decisions on the microscopic scale is betrayed by the long time dynamics, forming dynamic dependencies that break macroscopic rationality. Their choices create a point of structural instability that is sensitive to perturbation beyond all orders of modelable precision, and as the macroscopic behaviour falls on a dynamic attractor inflicted by this instability, a unique outcome becomes indeterminable.

In fig. 2 in particular, we saw what happened if the pilot's decisions failed to be precisely simultaneous, resulting in entirely different forward motions. This poses a particular problem in a variety of practical scenarios, as there may exist no unique absolute sequencing of decisions. If there is physical separation between decision makers and their apparatus, then the perceived sequencing of decisions at different places in the system is relative, depending on the distances involved and the speed of information travel, for example between the pilots, their controls, and their sensors.

To help visualize this we can represent the pilot scenario as a transport problem. Consider two raw materials produced at rates u and v, from separate mines M_u and M_v. These are sent to either of two factories, F_u and F_v, for processing, namely M_u is sent to F_u, and M_v to F_v, at times of low production denoted by $\lambda_u = 0$ and $\lambda_v = 0$. When production at M_u is high, denoted $\lambda_u = 1$, its material is routed through both factories, and similarly for M_v when $\lambda_v = 1$. The processed materials are manufactured into a final product at rate w. The equation (2) describes the state of the network at any instant, and (3) describes how this causes the network — the rates of mining and manufacture — to evolve. Because the system is evolving, then under the conditions reached in the pilots' dilemma, its behaviour becomes indeterminate, and the rational expectation of behaviour based on the static state (2) becomes meaningless for determining, for example, an optimal transport strategy.

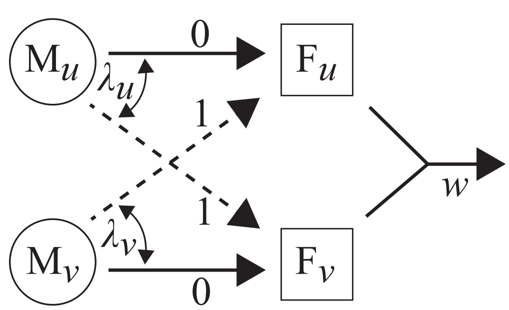

FIG. 8. Schematic of a transport network for the pilots' dilemma.

The resources in question may indeed be physical materials or packages, being routed across a network of processing stations towards their ultimate destinations, by what appears at any instant to be the most effective path. They may be electronic in nature, whether carrying power across machines or grids, or sending electronic instructions to send control actions or investment and trade decisions. In many such systems the high speeds of decision making versus the physical scales mean that simultaneity, and therefore unique sequencing, of decisions become impossible to define, as discussed in [6] for example.

Being neither chaotic nor stochastic, the indeterminacy here is not one commonly dealt with in dynamical systems literature. So can we look elsewhere for similar forms of behaviour that might provide insight?

Quantum mechanics may seem an extreme place to look for comparison, but Schrödinger's cat thought experiment provides a useful cnouterpoint. In this, a cat's fate is made uncertain due to the fundamentally probabilistic evolution of a wave function. In our pilots' dilemma the system is fundamentally deterministic, yet that determinacy is broken over time by the discontinuities in the microscopic interaction of the pilots' decisions. Their similarity is that in both cases the indeterminacy is rooted in a problem of singular perturbations. In quantum mechanics the limit $\hbar \to 0$ is singular, and for small $\hbar$ and a body (like a cat) of large mass, any miniscule perturbation will cause a probabilistic wave solution to collapse to a definite classical state (see e.g. [4, 15, 16]). In the pilots' dilemma the singular limit concerned is the smallness of the ε-neighbourhood of states around which the decisions are made. In the singular limit a range of outcomes are possible, and any slight alteration in assumptions of how the decisions proceed selects one of the infinitely many possiblities.

Such ambiguities are nothing new in *static* problems, particularly in rigid body problems. The forces through seemingly simple arrangements of bodies are unsolvable, like a ladder leaning against a wall (at a shallow angle), or a stool with more than three legs resting on a floor (making wobbling chairs and tables on uneven floors so commonplace). These are typically cited only as examples to avoid. To resolve them requires precise knowledge of the compliance of the bodiies and the contact between them, meaning in effect, even for such simple physical set ups, there are no 'typical' ladders or stools or floors about which to make general statements.

A more subtle conceptual counterpoint is Bertrand's chord paradox (see e.g. [1, 5, 19]). Given a circle inscribed with an equilateral triangle, what is the probablity that a chord of the circle has length larger than the side length of the triangle? Somewhat surprisingly, Joseph Bertrand showed that the answer is not unique. It turns out that the probability depends on the method by which the chord is chosen: again there is no 'typical' answer to the problem.

The pilots' dilemma is no different to these, showing us an indeterminacy resolvable only by perfect knowledge of the processes and sequences of decision making. Those processes are often complex and poorly understood, and may in fact be impossible to resolve at all. When the indeterminacy affects the kind of attractor an evolving system will follow, its consequences for applications become non-trivial.

One can find equations with discontinuous righthand sides of the form (3) scattered through models of rigid body mechanics, economics, predator-prey systems, electronic control, circuits with superconducting elements, cell biology and genetics, climate, . . . too many to review here (see e.g. [7, 12] as a starting point, or search for papers mentioning dynamics of *nonsmooth, piecewise, Filippov, sliding, or discontinuous* type). They may describe decisions and control actions, or represent changes in medium or environment. They seem to be rapidly rising in usage in mathematical modeling, partly because they offer piecewise-linear simplifications of insoluble nonlinear models, and partly because of the deceptive ease of encoding such discontinuities into numerical simulations. A single decision or discontinuity can create ambiguities (see [11, 12]), but not with such extreme effects as arise with two or more discontinuities as seen here. Though a number of methods have been proposed for resolving the dynamics at an intersection of discontinuities (e.g. [2, 3, 8, 9, 14, 17]), they are unable to escape the ambiguity that confronts them all. Indeed the reason why this has not come to light before is simple enough — it involves decision processes, which mathematically are 'discontinuous', and invite a host of mathematical methods which, as we have shown, while appearing rigorous in isolation, when brought together could not be more contradictory.

In summary, we have revealed here a form of indeterminacy, of potential relevance wherever decisions or regulatory processes are involved, and we have tried to set out the particular conditions under which it occurs. We see here that rather than trying to resolve the indeterminacy, it is the indeterminacy itself that reveals the most interesting result after all: a localized, non-chaotic, non-stochastic, classical (i.e. non-quantum) source of uncertainty.

---

[1] D. Aerts and M. S. de Bianchi. Solving the hard problem of Bertrand's paradox. *J Math Phys*, 55(083503):1–17, 2014.

[2] J. C. Alexander and T. I. Seidman. Sliding modes in intersecting switching surfaces, I: Blending. *Houston J. Math*, 24(3):545–569, 1998.

[3] J. C. Alexander and T. I. Seidman. Sliding modes in intersecting switching surfaces, II: Hysteresis. *Houston J. Math*, 25(1):185–211, 1999.

[4] M. V. Berry. Singular limits. *Physics Today*, 55(5 May 2002):10–11, 2002.

[5] J. Bertrand. Calcul des probabilités. *Gauthier-Villars*, pages 5–6, 1889.

[6] J. Cartwright. Time traders. *Physics World*, 31(7):24–27, 2018.

[7] M. di Bernardo, C. J. Budd, A. R. Champneys, and P. Kowalczyk. *Piecewise-Smooth Dynamical Systems: Theory and Applications*. Springer, 2008.

[8] L. Dieci and F. Difonzo. A comparison of Filippov sliding vector fields in codimension 2. *Journal of Computational and Applied Mathematics*, 262:161 – 179, 2014.

[9] L. Dieci and L. Lopez. Sliding motion on discontinuity surfaces of high co-dimension. a construction for selecting a Filippov vector field. *Numer. Math.*, 117:779–811, 2011.

[10] D. Gale. Dynamics coordination games. *Econ. Theory*, 5:1–18, 1995.

[11] M. R. Jeffrey. The ghosts of departed quantities in switches and transitions. *SIAM Review*, 60(1):116–36, 2017.

[12] M. R. Jeffrey. *Hidden Dynamics: The mathematics of switches, decisions, & other discontinuous behaviour*. Springer, 2019.

[13] M. R. Jeffrey. *Modeling with nonsmooth dynamics*. Frontiers in Applied Dynamical Systems. Springer Nature Switzerland, 2020.

[14] M. R. Jeffrey, G. Kafanas, and D. J. W. Simpson. Jitter in dynamical systems with intersecting discontinuity surfaces. *IJBC*, 28(6):1–22, 2018.

[15] G. Jona-Lasinio, F. Martinelli, and E. Scoppola. New approach to the semiclassical limit of quantum mechanics. *Commun. Math. Phys.*, 80:223–54, 1981.

[16] G. Jona-Lasinio, F. Martinelli, and E. Scoppola. The semiclassical limit of quantum mechanics: A qualitative theory via stochastic mechanics. *Phys. Rep.*, 77:313–27, 1981.

[17] J. Llibre, P. R. da Silva, and M. A. Teixeira. Sliding vector fields for non-smooth dynamical systems having intersecting switching manifolds. *Nonlinearity*, 28(2):493–507, 2015.

[18] G. Owen. *Game Theory*. Academic Press, 1995.

[19] D. P. Rowbottom. Bertrand's paradox revisited: Why Bertrand's 'solutions' are all inapplicable. *Philos. Math. (III)*, 21:110–114, 2013.

[20] E. Schrödinger. Die gegenwärtige Situation in der Quantenmechanik. *Naturwissenschaften*, 23(48):807–812, 1935.

[21] D. J. W. Simpson. Border-collision bifurcations in R^n. *SIAM Review*, 58(2):177–226, 2016.